

A method for comparing discrete kinematic data and N -body simulations

Prasenjit Saha¹

Mount Stromlo and Siding Spring Observatories,
Australian National University,
Canberra ACT 0200, Australia

This paper describes a method for quantitatively comparing an N -body model with a sample of discrete kinematic data. The comparison has two stages: (i) finding the optimum scaling and orientation of the model relative to the data; and (ii) calculating a goodness of fit, and hence assessing the plausibility of the model in view of the data.

The method derives from considering the data and model both as samples from some underlying binned distribution function, and applying probability theory arguments.

As an example, I consider a published N -body model for the Galactic bulge and disc, and fictitious l, b, v measurements, and recover (with error estimates) the spatial and velocity scales of the model and the orientation of the bar. The fictitious data are actually derived from the model by assuming the mass scale and the solar position, but their size and extent mimics a recent survey of OH/IR stars. The results indicate that mass of the bulge and our viewing angle of the bar are usefully estimable from current surveys.

¹ Present address: Department of Physics (Astrophysics), Keble Road, Oxford OX1 3RH, United Kingdom. Email: saha@physics.ox.ac.uk

1. INTRODUCTION

Kinematic surveys of a population of discrete objects are an increasingly important kind of data in galactic astronomy. The objects may be stars in globular clusters or elsewhere in the Galaxy (e.g., Meylan & Mayor 1986), emission line objects in the Galaxy or other galaxies (e.g., Ciardullo *et al.* 1993, Hui 1993, Arnaboldi *et al.* 1994, Tremblay *et al.* 1995, Beaulieu 1996, Sevenster *et al.* 1997a,b), or galaxies in a cluster (e.g., Colless & Dunn 1996). Such surveys usually measure sky positions and line-of-sight velocities, but for some systems proper motions are also available (e.g., Spaenhauer *et al.* 1992).

One would like to be able to throw these data at some dynamical analysis machine and reap all the dynamical results implicit in the data, but there is no such machine. Some progress towards this goal has been made, notably by D. Merritt and collaborators (see Merritt 1993, Merritt & Tremblay 1993, Merritt & Gebhardt 1994, and especially Merritt 1996). These papers develop methods for reconstructing mass profiles (including dark matter) from kinematical observations, in a model independent way. But at present they extend only to axisymmetric systems viewed in the equatorial plane. So for triaxial systems, and certainly for non-equilibrium systems like clusters of galaxies, it is basically N -body simulations that have to be confronted with data. How can we best do this quantitatively?

Generally speaking, there are three questions one would like answers to when comparing N -body models with observations.

- (i) How should a model be scaled and oriented to best fit the data?
- (ii) Could the data at hand have plausibly come from a particular model's distribution, or do the data rule out the model?
- (iii) If there are several plausible models, which one do the data favor?

All three are answerable if we can calculate the likelihood function, which is the probability of having gathered the actual data under a particular model. Suppose for definiteness that the data consist of measurements of sky position l, b , and line-of-sight velocity v , with negligible errors. Let us also assume for now that the simulation is so fine grained that it effectively gives us a distribution function f . One usually thinks of f as a function of phase space variables, but we can change variables to express it as $f(l, b, v, \eta)$, where η stands for three unmeasured numbers (e.g., distance and proper motion). Then the probability of drawing values l_k, b_k, v_k from f is

$$\text{prob}(l_k, b_k, v_k | f) = \int f(l_k, b_k, v_k, \eta) d\eta. \quad (1)$$

Assuming the data on different objects are independent, we have for the likelihood:

$$\text{prob}(\text{data} | f) = \prod_k \left[\int f(l_k, b_k, v_k, \eta) d\eta \right]. \quad (2)$$

Since $f(l, b, v, \eta)$ will depend on the scalings and orientation adopted, we can fit for these parameters—the peak of $\text{prob}(\text{data} | f)$ in the relevant parameter space estimates the parameters and the broadness of that peak gives uncertainties. To answer question (ii), we

2 Comparing discrete kinematics and simulations

can test if the value of $\text{prob}(\text{data}|f)$ is typical of random data sets drawn for that f ; if $\text{prob}(\text{data}|f)$ is anomalously low, we can infer that f is inconsistent with the data. Question (iii) can be answered by comparing $\text{prob}(\text{data}|f)$ for the various models available; there is an extra complication though, in that we must marginalize over the parameters for each model—see Sivia (1996) for a discussion of this point. I will not address model comparison in this paper.

The contribution of this paper is to derive and test a practical approximation to the ‘in-principle’ procedure above. We need an approximation because particle simulations do not give us f directly; we need to smooth somehow. Smoothings in general introduce biases, so we have to monitor for biases and correct for them if necessary. But bearing that caution in mind, the smoothing I propose to use is the simple-minded one of just binning in l, b, v , i.e., assuming that f is constant within boxes in l, b, v space. Let us say that for some choice of scaling and orientation parameters, the i -th bin has m_i model points and s_i data object points; also let $M = \sum_i m_i$ and $S = \sum_i s_i$. This immediately suggests minimizing χ^2 to obtain a best fit, but that is a bad idea. Minimizing χ^2 implicitly assumes that the s_i follow a Gaussian distribution, the mean and variance in this case being both equal to $m_i S/M$. This is fine if all the $s_i \gg 1$, but S being typically dozens to hundreds we do not have such luxury. Moreover, for bin sizes of interest, even the m_i may not always be large enough for shot noise to be negligible. The solution is to view *both* the sets m_i and s_i as samples drawn from some underlying f that is constant within bins. The likelihood then takes the form

$$\text{prob}(\text{data}|\text{model}) \propto W = \prod_{i=1}^B \frac{(m_i + s_i)!}{m_i! s_i!}. \quad (3)$$

This formula is derived in the Appendix, but note two intuitively desirable properties of W : (i) the $(m_i + s_i)!$ factor favors large m_i coinciding with large s_i , but the denominator discourages extremes like $m_i = M$ at the bin with highest s_i and 0 elsewhere; and (ii) if some outlier observation lands in a bin with no model points (i.e., $m_i = 0, s_i = 1$), that bin contributes unity to the product—in this sense W is robust against outliers.

Although the formula (3) is symmetric in m_i and s_i , operationally these two sets of numbers will play quite different roles. The s_i derive from data and, for a given data set and binning, they are fixed. The m_i , on the other hand, depend on the scaling and orientation parameters and will vary as those parameters are adjusted to maximize W .

To explain the details of the use of W it is probably best to work through an example, and below we work through the problem of scaling and orienting N -body models of the Milky Way bulge and inner disc from l, b, v measurements. As it happened, it was this problem that led to the present work, but the bulge is a good example to illustrate anyway, for two reasons. Firstly, it is a triaxial system with the interesting complication that its depth is not negligible compared to its distance. Secondly, there are several both of data sets (te Lintel Hekkert *et al.* 1991, Beaulieu 1996, Sevenster *et al.* 1997a,b) and models (Sellwood 1993, Zhao 1996, Fux 1997) in the recent literature.

2. EXAMPLE: SELLWOOD'S GALACTIC MODEL

Figure 1 shows an N -body model of the Galaxy by Sellwood (1993). Note the bar in the bulge, which makes the bulge triaxial. The real Galactic bulge is now generally agreed to have a substantial bar (oriented such that the side nearer to us is receding); see Gerhard (1996) for a review. Hence the interest of comparing models such as Sellwood's with kinematic data.

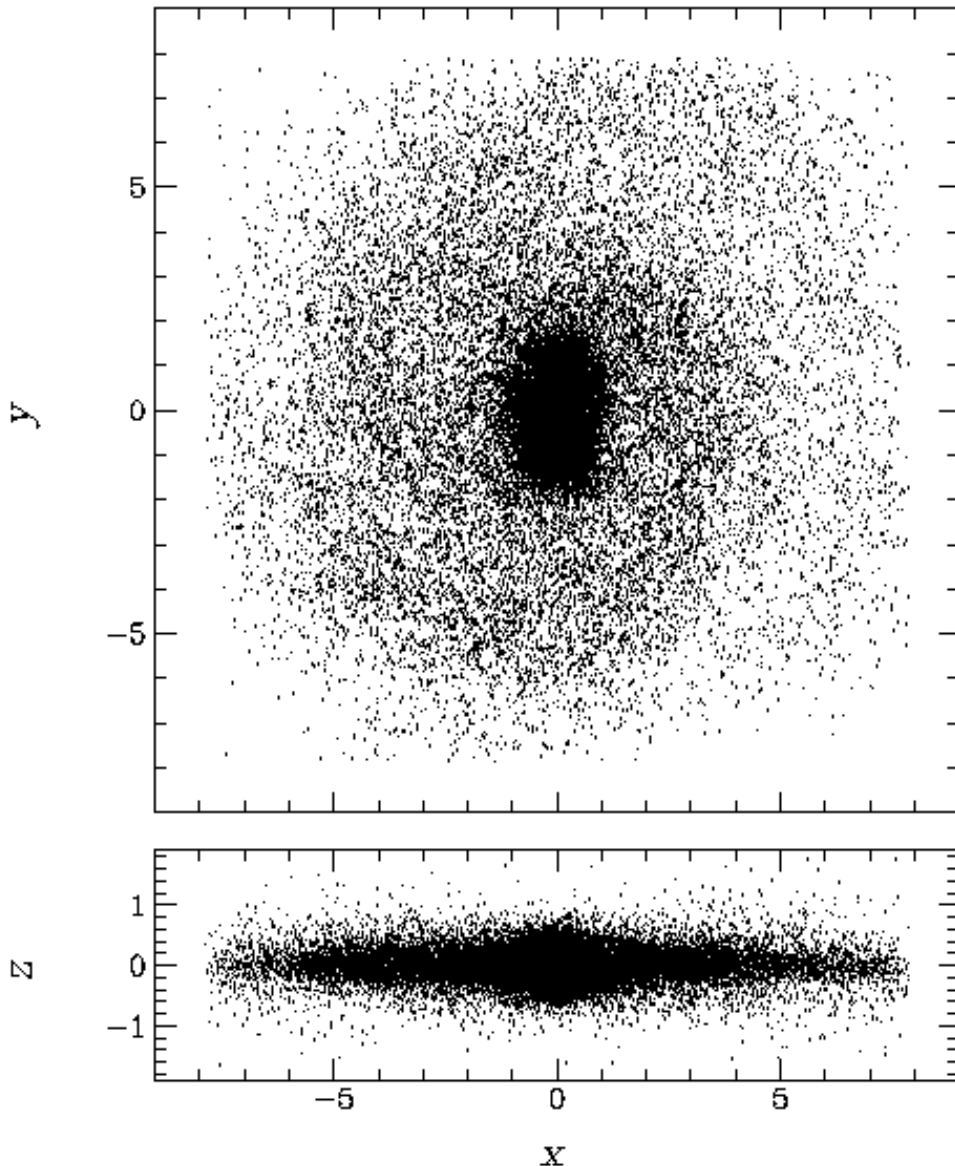


Figure 1. Spatial positions of 43802 particles in Sellwood's (1993) model for the Galaxy. As the spiral arms in the upper panel suggest, the model rotates counterclockwise, so positive z corresponds to the South Galactic direction. The mock l, b, v data are generated by viewing the particles from a 7 o'clock position on the (x, y) plane at radius of 6.

4 Comparing discrete kinematics and simulations

Let us put ourselves at the point $(-R_0 \sin \varphi, R_0 \cos \varphi, 0)$ in the N -body model and look towards the bulge. To evaluate the observed quantities from this location, we rotate and scale the model thus:

$$\begin{aligned}
 x' &= x \cos \varphi - y \sin \varphi \\
 y' &= x \sin \varphi + y \cos \varphi + R_0 \\
 z' &= z \\
 v'_x &= v_{\text{scale}}(v_x \cos \varphi - v_y \sin \varphi) - v_0 \\
 v'_y &= v_{\text{scale}}(v_x \sin \varphi + v_y \cos \varphi) \\
 v'_z &= v_{\text{scale}}v_z
 \end{aligned} \tag{4}$$

and then compute

$$\begin{aligned}
 r'^2 &= x'^2 + y'^2 + z'^2 \\
 l &= \arctan(y', x') \\
 b &= \arcsin(z'/r') \\
 v &= (x'v_{x'} + y'v_{y'} + z'v_{z'})/r'.
 \end{aligned} \tag{5}$$

Here R_0 is our Galactocentric radius in model units (Sellwood suggests $R \simeq 6$), v_{scale} is the scaling factor between real and model velocity units, v_0 is our tangential velocity in real units, φ is the viewing angle of the bar, and our radial velocity is assumed 0 or corrected for. In the convention implied by equations (4) and (5), φ between 0 and 90° means that the nearer side of the bar is at positive l and (because the model has positive rotation) positive v . The real Galactic bar is believed to be in such an orientation.

The asymmetry between the spatial and velocity parts of equation (4) may seem odd—why not

$$\begin{aligned}
 x' &= r_{\text{scale}}(x \cos \varphi - y \sin \varphi) \\
 y' &= r_{\text{scale}}(x \sin \varphi + y \cos \varphi) + R_0 \\
 z' &= r_{\text{scale}}z?
 \end{aligned} \tag{6}$$

We *would* need an extra parameter r_{scale} if we were considering proper motion data (available for Baade's window stars in Spaenhauer *et al.* 1992). But from equation (5) the observables all depend only on the ratio R_0/r_{scale} , so in equation (4) we drop r_{scale} . Then R_0 in effect becomes a surrogate for the spatial scale: if our true Galactocentric distance is 8.5 kpc then

$$r_{\text{scale}} = \left(\frac{8.5}{R_0} \right) \left(\frac{\text{kpc}}{\text{model unit}} \right).$$

With proper motion data, in principle r_{scale} and R_0 could both be determined, thus providing the actual Galactocentric distance; but with only l, b, v that distance must be supplied separately to get r_{scale} . Once we have r_{scale} , we can get the mass because the scale for $G \times \text{mass}$ is $r_{\text{scale}} \times v_{\text{scale}}^2$ (since GM has dimensions of L^3T^{-2}).

Consider now a survey of l, b, v measurements, which we would like to compare with the simulation and infer $R_0, \varphi, v_{\text{scale}}$, and v_0 to the extent possible. The first step is

to choose the bins in l, b, v for comparison—more on choosing bins below, but for the moment suppose we have chosen our B bins. This sets the s_i . The m_i will depend on what scaling and orientation parameters we choose; for any choice we can put the model particles through the transformations (4) and (5), bin them up, and randomly pick M out of all the particles that fall into our B bins, thus getting the m_i . Then we calculate W , which clearly depends on the parameters.¹ Clearly, our strategy to estimate the parameters will be to vary them so as to maximize W . Getting error bars and testing the model are a little more involved, and discussed in detail in Section 3. They will involve simulating data sets from the model. Generating a simulated data set s_i from the model is like generating m_i , except that we choose S particles rather than M . Sometimes we will be calculating W for two sets of occupancies s_i and m_i , both of which come from the model, but using different parameter values.²

How to choose the bins? Because of the assumptions that go into the derivation of W , it is best to avoid unequally sized bins. But there is no need to have bins in unsurveyed regions, so bins need not be contiguous. The bin size requires some thought. I cannot suggest any definite prescription for the bin size, but there are two guidelines. Firstly, B should be several times smaller than M , so that the m_i can be large enough to actually carry some information about the distribution function; $B \simeq M/5$ seems serviceable. There is no problem with $B \gg S$; after all, the continuous limit is $M \gg B \gg S$. Secondly, the binning should not be so coarse that it misses important features in the distribution function. Too coarse a binning can lead to strange biases, as the following suggests. The scale height of the bulge (as seen from the solar system) is about 2.2° ; suppose the bins were 5° in b . When fed data binned thus, any model fitting procedure is likely to respond by fitting a model with an increased scale in b . An easy way to do this is to increase R_0 —but then the fit would have to compensate for the scale in l , which it might do by reducing φ to make the bar more nearly end-on; but a nearly end-on bar will tend to give larger v values, and this in turn might be compensated by reducing v_{scale} .

¹ The number of model particles that fall into our B bins will depend on the parameters. Particles may fall outside the survey region where we might have no bins. But M must be kept the same for all parameter values, i.e., we must always choose a subset of size M of those model particles that *do* fall into our B bins. Otherwise the formula (3) for W becomes invalid (see the Appendix).

² If we are going to compare mock data generated from a model with that model, it is important to then remove from the model those points which went into the mock data. A model particle should never contribute to both s_i and m_j at the same time. The reason is that the data are not supposed to correspond *exactly* to any model particles, only to have come from the same distribution function.

3. USE OF THE W FUNCTION

It is straightforward to incorporate the likelihood W in standard Monte-Carlo procedures for parameter estimation and model testing, and the following describes how this can be done. The approach here is not the only possible one, and Bayesian purists would reject it entirely; but it seems computationally the most tractable.

It is helpful to consider two functions, D and Ω .

$D(\omega)$ is a function that generates a data set from the model using parameter values ω . D is probabilistic, so there can be many possible data sets $D_1, D_2, \dots(\omega)$ from the same model and parameters. If the model is correct and the true values are ω_{true} , then the observed data can be thought of as one realization of D :

$$D_{\text{obs}} = D(\omega_{\text{true}}). \quad (7)$$

W depends on both the data and the parameters:

$$W = W(D, \omega') \quad \text{or} : W(D(\omega), \omega'). \quad (8)$$

In general $\omega' \neq \omega$; ω leads to the data and hence to the s_i , but the m_i are got by applying a possibly different value ω' to the model. We now define the function Ω thus:

$$\Omega(D) = \omega' : W(D, \omega') \text{ is maximum.} \quad (9)$$

To calculate $\Omega(D)$, we don't need to know what ω value gave D ; but $\Omega(D)$ is an estimator for that unknown value (in fact, a maximum likelihood estimator, because W is a likelihood).³

To estimate parameters we calculate $\omega_{\text{est}} = \Omega(D_{\text{obs}})$. For error bars on ω_{est} we want the scatter in $\Omega(D(\omega_{\text{true}}))$. But since in real applications we won't know ω_{true} , we can take instead the scatter in $\Omega(D(\omega_{\text{est}}))$; from this we can read off desired confidence limits. This is standard Monte-Carlo error estimation—see Figures 15.6.1 and 15.6.2 in *Numerical Recipes* by Press *et al.* (1992).

Testing the model is a little more complicated. We need some statistic that measures the goodness of a parameter fit, but the well known ones do not help us: χ^2 is inappropriate for the reasons given in Section 1, and KS and its relatives are inapplicable because the data are not one-dimensional. However, there is an obvious choice of statistic: W itself. To apply it, we compare $W(D_{\text{obs}}, \omega_{\text{est}})$ with the distribution of $W(D(\omega_{\text{true}}), \omega_{\text{est}})$. If $W(D_{\text{obs}}, \omega_{\text{est}})$ lies in the lowest percentile of the distribution of $W(D(\omega_{\text{true}}), \omega_{\text{est}})$, then the model is rejected at 99% significance, and so on. For χ^2 and also for KS and its

³ If we had

$$\langle \Omega(D(\omega)) \rangle = \omega,$$

(the average being over an ensemble of D_n with ω held fixed) then Ω would be an unbiased estimator. As suggested in Section 1, in practice Ω will have some bias, because for one thing the binning process introduces bias. But that is not a problem provided we can test for bias and correct for it where required.

relatives, the distribution corresponding to $W(D(\omega_{\text{true}}), \omega_{\text{est}})$ is model independent. In our case we will need to calculate the distribution; but again, we won't know ω_{est} , so we will have to substitute the distribution of $W(D(\omega_{\text{est}}), \omega_{\text{est}})$.

Note that if the goodness of fit test leads to rejection of the model, parameter estimates from that model must be rejected too (even if the error bars claim high accuracy).

The main algorithmic problem is locating the maximum of W in the multi-dimensional parameter space of ω . My implementation basically follows Charbonneau (1995). Programs are available to anyone interested.

4. SIMULATIONS WITH SELLWOOD'S MODEL

In this section I present some Monte-Carlo simulations to gain some idea of which bulge parameters can be constrained from current surveys and how well.

Consider Sellwood's model with ω_{true} being $R_0 = 6$ model units, $\varphi = 30^\circ$, $v_0 = 220$ km/sec, and $v_{\text{scale}} = 300$ km/sec/model unit. All these are plausible values, and using them I computed $\Omega(D(\omega_{\text{true}}))$ for 32 mock surveys, each having 300 objects in the range $|l| < 10.5^\circ$, $|b| < 3.25^\circ$, $|v| < 320$ km/sec. The size and extent mimics the symmetric part of the survey of bulge OH/IR stars by Sevenster *et al.* (1997a,b). (The survey region need not be symmetric—see below.) I used $21 \times 13 \times 16$ bins in l, b, v . Figure 2 shows the results: the ranges of the axes in R_0, v_0 , and φ are the ranges I searched; for v_{scale} I searched the range 0–500.

Figure 3 shows a sort of direct visual data-model comparison for one (the first) of the mock surveys. Such plots are useful in checking for programming goofs, but otherwise there is not much information one can extract from them.

Figure 4 illustrates that the maximum of W of the first of the mock surveys is typical of the values should expect from this model, as expected since the mock survey came from the model. With real data such a plot would test whether the data could plausibly have come from the model being studied.

From the results in Figure 2, the medians and 68% range in $\Omega(D(\omega_{\text{true}}))$ are $\varphi = (29_{-7}^{+8})^\circ$, $v_{\text{scale}} = 290_{-33}^{+20}$. These numbers indicate the sort of bias and error bars we can expect from a survey of this size and extent. We see that v_{scale} can be estimated to $\sim 10\%$ and φ to $\sim 10^\circ$ with no need to correct for bias. On the other hand, we get no useful information on v_0 and R_0 . That v_0 is not constrained by such data is not surprising, since it almost perpendicular to what is measured. But the inability to infer R_0 is puzzling, especially considering the impressively tight constraint on φ . Evidently, we must use integrated light to estimate R_0 .

It is interesting to see what happens as the surveys get bigger. Figure 5 shows $\Omega(D(\omega_{\text{true}}))$ for mock surveys when the size is extended to 500 and the l range to $-45^\circ < l < 10.5^\circ$, which mimics the full size and extent of Sevenster *et al.*'s (1997a,b) OH/IR survey. We now find approximate medians and 68% ranges of $\varphi = (29_{-8}^{+8})^\circ$ and $v_{\text{scale}} = 290_{-11}^{+23}$, but the outliers are noticeably less distant. We also begin to notice a bias

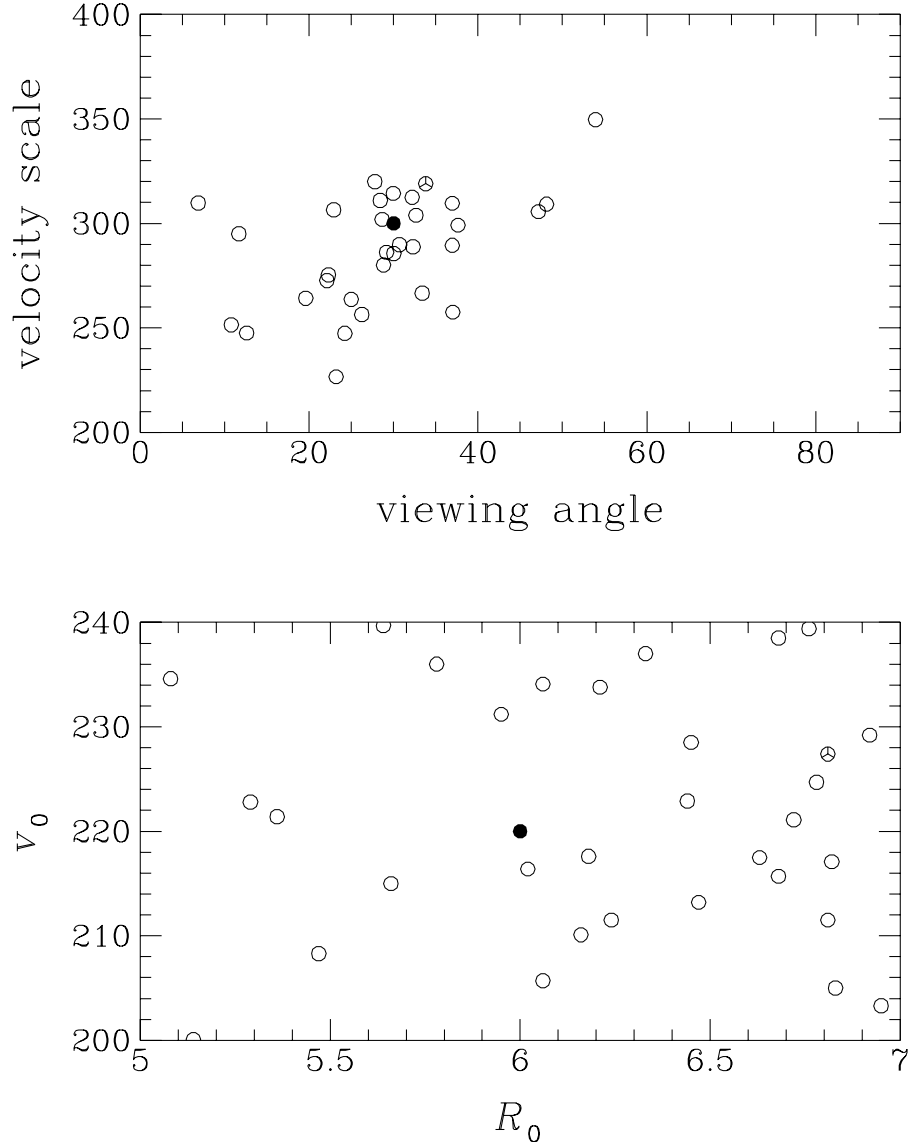


Figure 2. Recovery of parameter values from mock surveys of 300 objects in the range $|l| < 10.5^\circ$, $|b| < 3.25^\circ$. The filled circles show the parameter values used to generate the mock data, i.e., ω_{true} . The open circles show the parameters recovered from 32 different mock surveys, i.e., $\Omega(D_0..D_{31}(\omega_{\text{true}}))$. The open circles with three cuts inside refer to the mock survey $D_0(\omega_{\text{true}})$ that happened to be first; this D_0 is used again for Figures 3 and 4.

towards low estimates for v_{scale} and high estimates for R_0 ; if the survey size is increased further, the scatter in $\Omega(D(\omega_{\text{true}}))$ reduces further, and the biases in v_{scale} and R_0 become correspondingly more noticeable.

To summarize the results, these survey simulations indicate that current surveys can constrain the viewing angle of bulge simulations to $< 10^\circ$ and the velocity scale to $< 10\%$ (at 68% confidence). The spatial scales will need to be set independently using

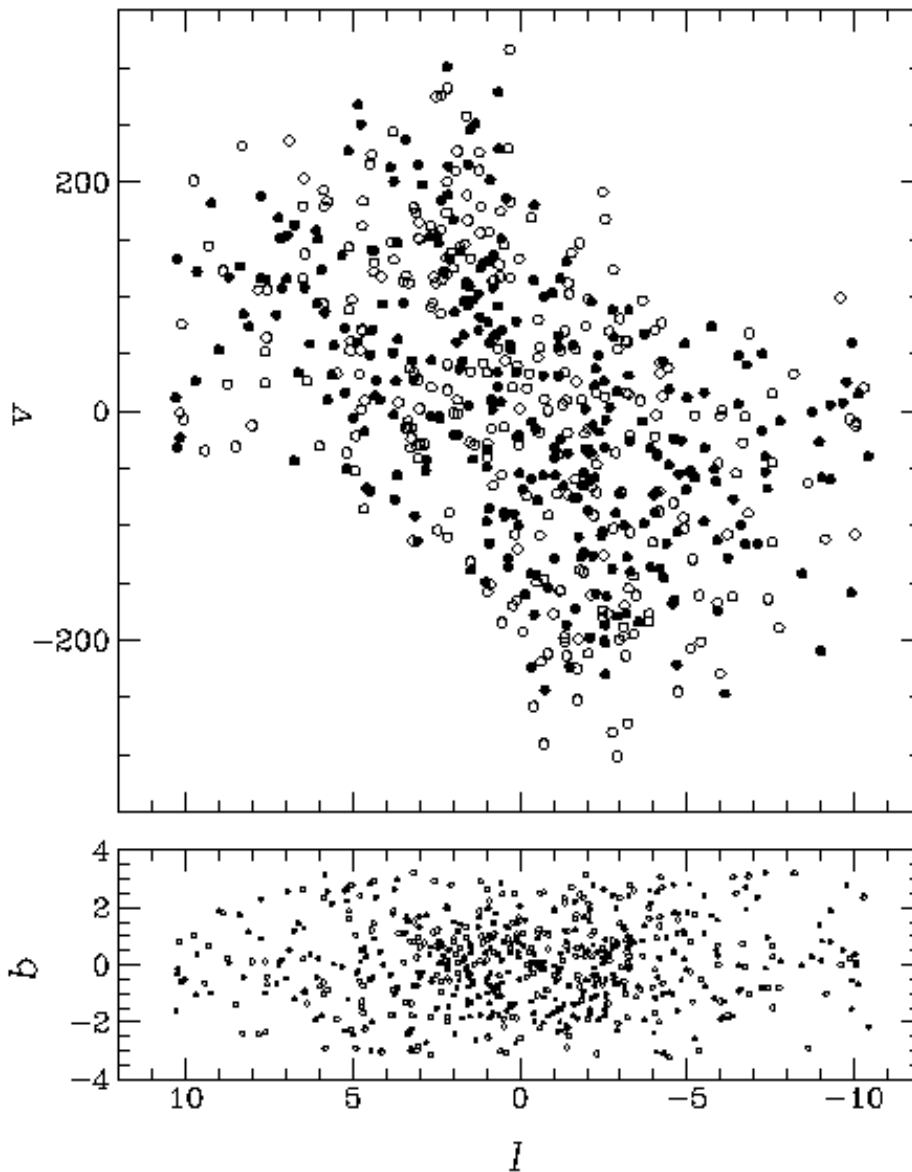


Figure 3. The open circles show l, b and l, v for a mock survey $D_0(\omega_{\text{true}})$. The filled circles show l, b and l, v for a mock survey $D_1(\omega_{\text{est}})$, where $\omega_{\text{est}} = \Omega(D_0(\omega_{\text{true}}))$. With a real survey one would use D_{obs} instead of $D_0(\omega_{\text{true}})$.

integrated light. Kalnajs (personal communication) obtains $\sim 10\%$ or better constraints on R_0 by comparing N -body models and integrated light from COBE. Combining with $< 10\%$ uncertainties on v_{scale} , it appears that N -body models could be scaled in mass to $\sim 25\%$. The resulting predictions for microlensing optical depths would easily be tight enough for interesting confrontations with bulge microlensing observations.

I am grateful to Ken Freeman for posing this problem and to Sylvie Beaulieu and Maartje Sevenster for teaching me about bulge observations. Thanks also to Agris Kalnajs and

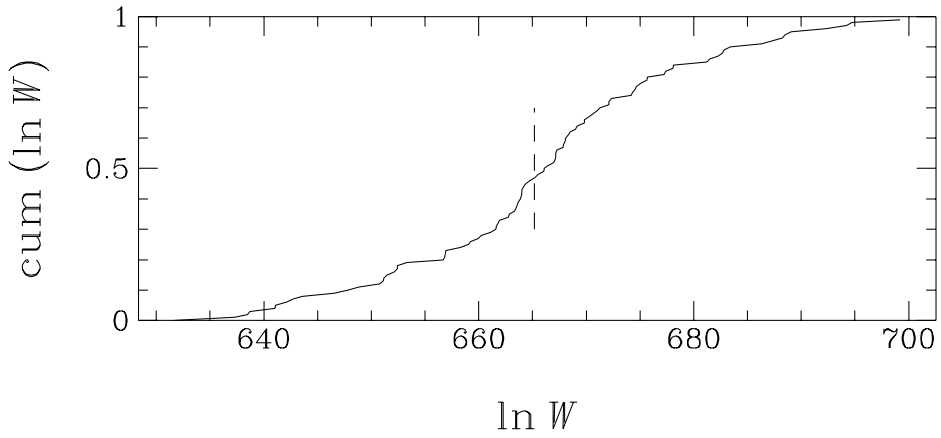


Figure 4. The vertical dashed line in this figure shows the value of $\ln W(D_0(\omega_{\text{true}}), \omega_{\text{est}})$ where $\omega_{\text{est}} = \Omega(D_0(\omega_{\text{true}}))$ which is marked in Figure 2. With a real survey $D_0(\omega_{\text{true}})$ would be replaced by D_{obs} . The rising curve is the cumulative distribution of $\ln W(D_1 \dots D_{100}(\omega_{\text{true}}), \omega_{\text{est}})$. As expected, $D_0(\omega_{\text{true}})$ appears as typical of the distribution $D_n(\omega_{\text{true}})$.

Maartje Sevenster for the appropriate mixture of enthusiasm and skepticism about W .

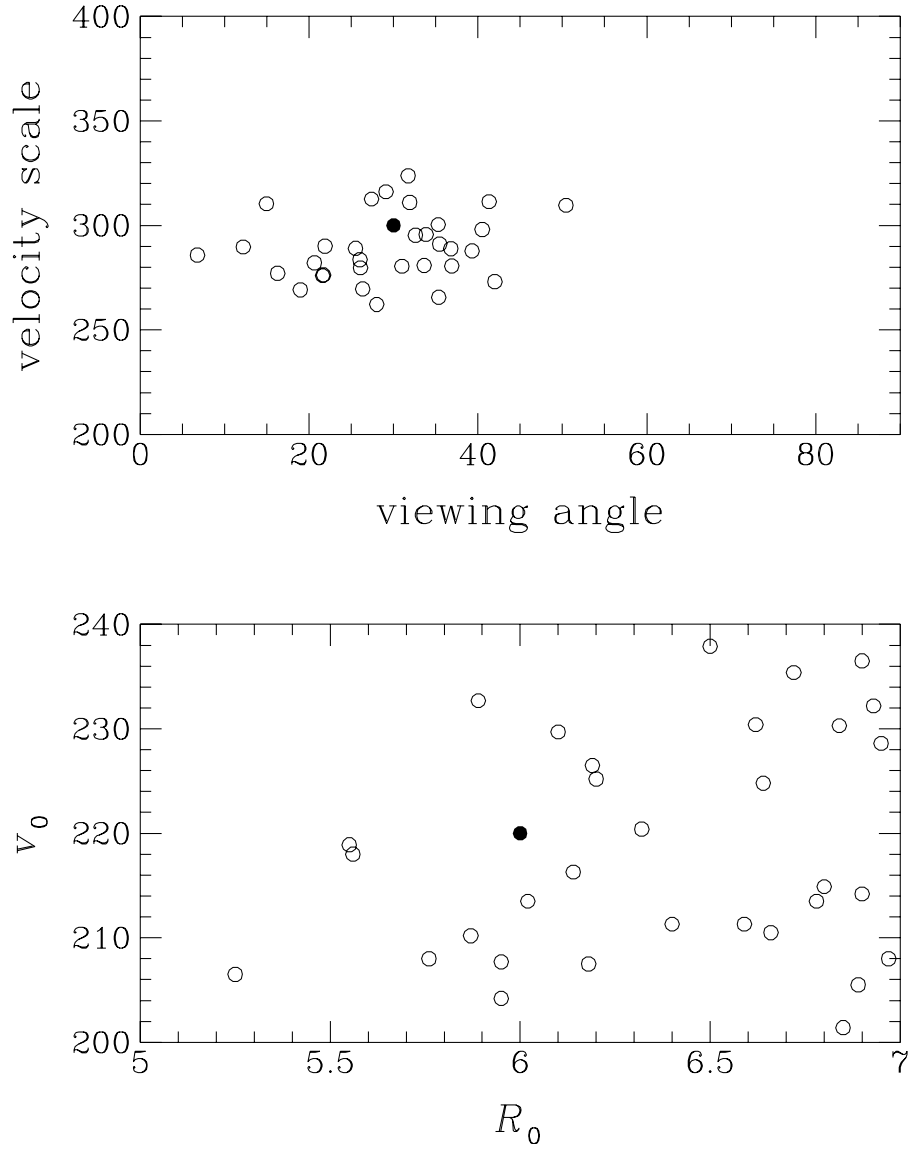


Figure 5. Similar to Figure 2, but this time the mock surveys have 500 objects each in the range $-45^\circ < l < 10.5^\circ$, $|b| < 3.25^\circ$.

REFERENCES

- Arnaboldi, M., Freeman, K.C., Hui, X., Capaccioli, M., & Ford, H. (1994) *ESO Messenger*, **76**, 40
- Beaulieu, S.F. (1996) Ph.D. thesis, Australian National University
- Charbonneau, P. (1995) *Astrophys. J. Supp.*, **101**, 309
- Ciardullo, R., Jacoby, G.H., Dejonghe, H.B. (1993) *Astrophys. J.*, **414**, 454
- Colless M. & Dunn A.M. (1996) *Astrophys. J.*, **458**, 435
- Fux, R. (1997) preprint, astro-ph/9706242
- Gerhard, O.E. (1996) in *Proc. AIU Symp. 169, Unsolved problems of the Milky Way*, ed. L. Blitz & P. Teuben (Reidel, Dordrecht)
- Hui, X. (1993) *Pub. Astron. Soc. Pacific.*, **105**, 1011
- te Lintel Hekkert, P., Caswell, J.L., Habing, H.J., Haynes, R.F., & Norris, R.P. (1991) *Astron. Astrophys. Supp.* **90**, 327
- Merritt, D. (1993) *Astrophys. J.*, **413**, 79
- Merritt, D. (1996) *Astron. J.*, **112**, 1085
- Merritt, D. & Gebhardt, K. (1994) in *Clusters of Galaxies, Proceedings of the XXIXth Rencontre de Moriond*, ed. F. Durret, A. Mazure & J. Trân Thanh Vân (Editions Frontiere: Singapore)
- Merritt, D. & Tremblay, B. (1993) *Astron. J.*, **106**, 2229
- Meylan, G. & Mayor, M. (1986) *Astron. Astrophys.*, **166**, 122
- Press, W.H., Teukolsky, S.A., Vetterling, W.T., & Flannery, B.P. (1992) *Numerical Recipes*, second ed. (CUP)
- Sellwood, J.A. (1993) in *Back to the Galaxy*, eds. Holt, S.S., & Verter, F. (AIP press)
- Sevenster, M.N., Chapman, J.M., Habing, H.J., Killeen, N.E.B., & Lindqvist, M. (1997a) *Astron. Astrophys. Supp*, **122**, 79
- Sevenster, M.N., Chapman, J.M., Habing, H.J., Killeen, N.E.B., & Lindqvist, M. (1997b) *Astron. Astrophys. Supp*, in press
- Sivia, D.S. (1996) *Data Analysis, A Bayesian Tutorial*, (OUP)
- Spaenhauer, A., Jones, B.F., & Whitford, A.E. (1992) *Astron. J.*, **103**, 297
- Tremblay, B., Merritt, D., & Williams, T.B. (1995), *Astrophys. J.*, **443**, L5
- Zhao H.S. (1996) *Mon. Not. Roy. astr. Soc.*, **283**, 149

APPENDIX

This appendix derives the likelihood formula (3) from probability theory arguments.

Continuing the notation of Section 1, we suppose that there are B bins in all, and that in the i -th bin $f = f_i$, and both m_i and s_i are drawn from f_i .

The joint probability for the bin occupancies is the product of two multinomial distributions:

$$\text{prob}(s_i, m_i | f_i) = M! S! \prod_{i=1}^B \frac{f_i^{m_i+s_i}}{m_i! s_i!}. \quad (\text{A1})$$

Equation (A1) could be used to estimate the f_i , with uncertainties. But as we have no particular interest in the f_i as such, we marginalize them out in the usual way, which is to integrate over all allowed values of the f_i —that means all combinations of values of the f_i between 0 and 1, subject to $\sum_i f_i = 1$. Distributions of f_i that most resemble the m_i and s_i will, according to (A1), contribute most to the integral. Marginalization is just an application of the additive rule for probabilities. Using the identity

$$\left(\prod_{i=1}^B \int f_i^{n_i} df_i \right) \delta\left(\sum_j f_j - 1\right) = \frac{1}{(N+B-1)!} \prod_{i=1}^B n_i! \quad (\text{A2})$$

we get

$$\text{prob}(s_i, m_i) = \frac{M! S! (B-1)!}{(M+S+B-1)!} \prod_{i=1}^B \frac{(m_i + s_i)!}{m_i! s_i!}. \quad (\text{A3})$$

Putting $S = 0$ in (A3) gives $\text{prob}(m_i)$, and hence

$$\text{prob}(s_i | m_i) = \frac{S! (M+B-1)!}{(M+S+B-1)!} \prod_{i=1}^B \frac{(m_i + s_i)!}{m_i! s_i!}. \quad (\text{A4})$$

If $B = 1$ then the probabilities in (A3) and (A4) become unity, as they should. For the sort of applications of interest in this paper M , S , and B are fixed, so we can ignore the normalization in (A4) and work only about W as defined in equation (3).

If M is large enough compared to S that $m_i + s_i \simeq m_i$ and (A4) simplifies to

$$\text{prob}(s_i | m_i) \propto \prod_i \frac{m_i^{s_i}}{s_i!}, \quad (\text{A5})$$

which amounts to saying that $f_i = m_i/M$ because the shot noise in the m_i is negligible. If M is large enough that we can make the bins so small that each $s_i = 0$ or 1, but still all $m_i \gg 1$, then (A5) simplifies further, to

$$\text{prob}(s_i | m_i) \propto \prod_{j:s_j=1} m_j, \quad (\text{A6})$$

which amounts to the formula (2) for the continuous case. Thus, (A4) has the expected large- m_i limits.